MOLEKUL
eISSN: 2503-0310

Articles
https://doi.org/10.20884/1.jm.2026.21.2.16859

Exploring the Efficacy of Halogenated Thioxanthone Derivatives Against Multidrug-Resistant Gram-Positive Bacteria: An In Silico and In Vitro Approach

Muhammad Badrul Huda[1], Faris Hermawan[2]*, Jumina Jumina[3], Yudhi Dwi Kurniawan[2], Muhammad Eka Prastya[2], Nicky Rahmana Putra[2], Andini Sundowo[2]

[1]Department of Chemistry, Faculty of Science and Mathematics, Diponegoro University, Tembalang, Semarang 50275, Indonesia
[2]Research Center for Pharmaceutical Ingredient and Traditional Medicine, National Research and Innovation Agency (BRIN), Tangerang Selatan, Banten, Indonesia
[3]Department of Chemistry, Faculty of Mathematics and Natural Sciences, Universitas Gadjah Mada, Yogyakarta, Indonesia

*Corresponding author email: fari025@brin.go.id

Received August 02, 2025; **Accepted** May 10, 2026; **Available online** July 20, 2026

ABSTRACT. This study conducts a comprehensive analysis of halogenated thioxanthone derivatives through molecular docking, molecular dynamics simulations, and antimicrobial evaluation. The molecular docking analysis against *Bacillus subtilis* protein demonstrated that the halogenated thioxanthone derivatives (TX1–TX6) exhibited binding energies ranging from −6.22 to −7.35 kcal/mol, in comparison to tetracycline, which displayed a binding energy of −6.63 kcal/mol. Furthermore, the docking study against dihydrofolate reductase (DHFR) *Staphylococcus aureus* revealed binding energies for these compounds ranging from −6.93 to −7.65 kcal/mol, whereas trimethoprim and tetracycline exhibited binding energies of −7.19 and −7.73 kcal/mol, respectively. The 100 ns molecular dynamics simulation indicated that 2,4-dichloro-1,3-dihydroxythioxanthone (TX3) and 2,4-dibromo-1,3-dihydroxythioxanthone (TX6) maintained significant stability when interacting with *B. subtilis* and DHFR *S. aureus* proteins. Compounds TX3 and TX6 were found to exhibit antibacterial activity against Gram-positive bacteria, *B. subtilis* strain M18, and methicillin-resistant *Staphylococcus aureus* (MRSA). Among the tested compounds, TX3 exhibited the highest antibacterial activity, with a MIC of 1.98 μg/mL and a MBC of 3.9 μg/mL. In comparison, TX6 demonstrated a MIC of 3.9 μg/mL and an MBC of 7.9 μg/mL. The tetracycline exhibited a MIC value of 3.9 μg/mL and an MBC value of 3.9 μg/mL.

Keywords: *Bacillus subtilis,* Molecular docking, Molecular dynamics, MRSA, Thioxanthone

INTRODUCTION

The rise of antibiotic-resistant bacteria has become a major global health crisis, contributing to millions of deaths each year. By 2030, an estimated 5.2 million deaths in the Western Pacific Region will be attributed to antibiotic-resistant bacterial infections (WHO, 2023). *Methicillin-resistant Staphylococcus aureus* (MRSA) and *Bacillus subtilis* species are notable bacteria responsible for hospital-acquired infections. The rising resistance to all current classes of antibiotics has made these infections increasingly challenging to manage (Asyraf et al., 2022). In recent years, infections resulting from drug-resistant strains of MRSA and *B. subtilis* have significantly elevated the risk of mortality (Lakhundi et al., 2018). Additionally, these types of bacteria have developed resistance to specific classes of antibiotics. *Staphylococcus aureus*, known to infect human skin and soft tissue, demonstrates resistance to methicillin (Bukharie et al., 2010). In contrast, *B. subtilis*, which is associated with cases of diarrhea, exhibits resistance to both ampicillin and gentamicin (Haque et al., 2024). Consequently, there is a critical necessity for developing novel, high-efficiency antibacterial agents and alternative strategies to address the gaps in the discovery and development of antibiotics.

Xanthones (9H-xanthen-9-one) represent a class of O-heterocyclic symmetrical compounds characterized by a dibenzo-γ-pyrone structural framework (Proenca et al., 2016). The structural modification of substituents on the xanthone rings, conducted through various chemical reactions, allows for the development of an extensive range of biological activities, including anticancer, antimalarial, antioxidant, anti-tuberculosis, antifungal, anti-inflammatory, and antibacterial (Iresha et al., 2022; Hastuti et al., 2024; Hermawan et al., 2024; Gampa et al., 2022; Librowski et al., 2005; Araujo et al., 2009; Lu et al., 2023). Thioxanthone, an isosteric analog of xanthone, consists of an S-heterocyclic core within a dibenzo-γ-thiopyrone scaffold (Nakagawa et al., 2020). In 2021, Duraes et al. conducted a

comprehensive study to evaluate the antibacterial efficacy of amine thioxanthone derivatives against four bacterial species: *Escherichia coli, Pseudomonas aeruginosa, Enterococcus faecalis*, and *S. aureus*. The study's findings demonstrated that the tested compounds exhibited a minimum inhibitory concentration (MIC) of 32 μg/mL against *E. faecalis* and *S. aureus* strains, highlighting their potential as antimicrobial agents (Duraes et al., 2021). Moreover, Bessa et al. (2015) demonstrated that thioxanthone derivatives functionalized with secondary amine and ester substituents exhibited potent antibacterial activity against MRSA and *B. subtilis*, with a minimum inhibitory concentration (MIC) of 64 μg/mL. In 2018, Resende et al. demonstrated that the inclusion of a chlorine atom within the xanthone structure displayed notable antibacterial activity against *E. faecalis* ATCC 29212 and *S. aureus* ATCC 29213 (Resende et al., 2018). Resende et al. (2020) reported that hydroxyxanthone with two bromo substituents plays a significant role in exhibiting antibacterial activity against *S. aureus* ATCC 29213.

Dihydrofolate reductase (DHFR) is an essential enzyme that facilitates the conversion of dihydrofolate to tetrahydrofolate. The inhibition of this enzyme disrupts DNA replication, which ultimately results in cell death (Pedrola et al., 2019). Pyrimidines, diaminopyrimidines, and analogous compounds are currently undergoing extensive research for their capacity to inhibit DHFR. This inhibition holds promise for the development of highly specific and potent anti-MRSA therapeutics (Kumar et al., 2023). The deletion of the *B. subtilis* LCP enzymes, namely TagTBS, TagUBS, and TagVBS, has been shown to have a lethal effect. The observed phenomenon is likely attributable to the accumulation of nonfunctional lipid-bound WTA intermediates, coupled with a deficiency in the lipid carriers essential for the synthesis of peptidoglycan (D'Elia et al., 2009; Kawai et al., 2011). In accordance with the findings presented, molecular docking and molecular dynamics simulations were employed to analyze the interactions and stability of halogenated thioxanthone derivatives with *B. subtilis* and DHFR *S. aureus* proteins, providing insights into their potential biological activity and binding affinity. The most potent compounds identified from in silico studies were further investigated for their antibacterial activity against the *B. subtilis* strain M18 and MRSA through experimental validation.

MATERIALS AND METHODS

Materials

The protein data bank website (www.rcsb.org) provided access to the X-ray crystal structures of *B. subtilis* (PDB ID: 6UF6) and DHFR *S. aureus* (PDB ID: 2W9H) proteins. Chimera software was used to isolate the target proteins, removing water molecules and cofactors from their structures. The three-dimensional (3D) structures of halogenated thioxanthone derivatives (**TX1**–**TX6**) were generated using Avogadro software and subsequently optimized using the Orca program. The optimization employed density functional theory (DFT) with the B3LYP 3-21G basis set, and the final structures were exported in .pdb file format. **Figure 1** illustrates the chemical structures of halogenated thioxanthone derivatives functionalized with hydroxy, chloro, and bromo substituents, which were utilized as ligands. Two clinical isolates, *B. subtilis* strain M18 and MRSA, have been obtained from Dr. Kariadi Central General Hospital in Semarang, Central Java, Indonesia. In addition, methanol p.a., media Mueller Hinton Broth (MHB; Oxoid), and McFarland standard 0.5 in 0.85% NaCl (Merck).

Molecular Docking Study

The protein complexes of *B. subtilis* (PDB ID: 6UF6) and the DHFR *S. aureus* (PDB ID: 2W9H) were obtained from the RCSB Protein Data Bank. The separation of protein and native ligand structures was performed using Chimera software, and the resulting files were saved in PDB format (Pettersen et al., 2004). The structures of the halogenated thioxanthone derivatives were constructed using Avogadro and optimized with the ORCA program at the DFT B3LYP/3-21G level. This level of theory was selected

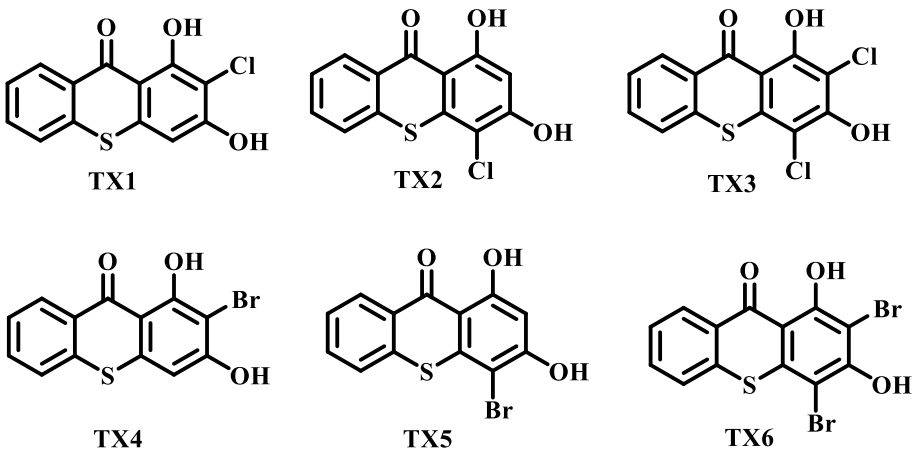

Figure 1. Chemical structure of the halogenated thioxanthone derivatives

based on our previous study, where B3LYP/3-21G showed the best method with experimental data for xanthone derivatives, confirming its reliability in describing molecular geometry and electronic properties (Neese et al., 2018). The optimized structures were then saved in .pdb format for further analysis (Fatmasari et al., 2025). Redocking and molecular docking simulations were performed using AutoDock4 with a grid box of 30 × 30 × 30 grid points and a grid spacing of 0.375 Å for both the B. subtilis (PDB ID: 6UF6) and DHFR S. aureus (PDB ID: 2W9H) proteins (Morris et al., 2009). The Lamarckian Genetic Algorithm (LGA) method was employed for 50 docking runs, and the resulting molecular docking outcomes were analyzed and visualized using Discovery Studio Visualizer (DSV) 2019 (Biovia 2009; Fuhrmann et al., 2010).

Molecular Dynamics Simulation

Molecular dynamics (MD) simulations of halogenated thioxanthone compounds were conducted using GROMACS 2023 software (Huang et al., 2013; Hess et al., 2008). The structural topology of *B. subtilis* and DHFR *S. aureus* proteins was generated using the CHARMM36 force field, while the topology parameters for all ligand molecules were derived using the CGenFF server. The protein–ligand complexes were placed in a cubic simulation box, solvated with TIP3P water molecules, neutralized by adding sodium ions, and subjected to periodic boundary conditions (PBC). To ensure system stability before subsequent simulations, energy minimization was performed using the steepest descent algorithm for a maximum of 50,000 steps until the maximum force converged below 1000 kJ mol^{-1} nm^{-1}. A sequential two-step equilibration process, each phase lasting 100 ps, was performed to achieve system stabilization under controlled thermodynamic conditions of 300 K temperature and 1 atm pressure. Initially, equilibration was performed within the NVT ensemble to maintain a fixed number of particles, volume, and temperature, followed by the NPT ensemble to regulate particle count, pressure, and temperature. Temperature coupling was maintained using the V-rescale thermostat, whereas pressure coupling was controlled using the C-rescale barostat (Bussi et al., 2007; Bernetti et al., 2020). Utilizing the Particle Mesh Ewald (PME) method allowed efficient calculation of electrostatic interactions over long distances while preserving system homogeneity (Darden et al., 1993). The molecular dynamics simulation was subsequently conducted for 100 ns, ensuring a stable temperature of 300 K and a pressure of 1 bar. The MD simulation results were quantitatively analyzed through graphical representations of Root Mean Square Deviation (RMSD), Root Mean Square Fluctuation (RMSF), and Radius of Gyration (Rg) to evaluate system stability and conformational changes.

Antimicrobial Activity

The antibacterial efficacy of the samples was evaluated through the determination of Minimum Inhibitory Concentration (MIC) and Minimum Bactericidal Concentration (MBC) values, employing the micro broth dilution method (Putra et al., 2024). A range of sample concentrations from 3.9 μg/mL to 500 μg/mL was prepared by dilution with methanol p.a (Sigma) and dispensed into a sterile 96-well plate (Biologix). The prepared sample concentrations were mixed with Mueller-Hinton Broth (MHB; Oxoid) until a total volume of 100 μL was attained. Following the cultivation of the bacterial samples for 24 hours, 100 μL from each test culture was adjusted to a McFarland standard of 0.5 using 0.85% NaCl (Merck), corresponding to 10^8 CFU/mL of bacteria. This preparation was then added to each well and incubated for 24 hours in a shaker incubator set at 150 rpm and a temperature of 37 ºC. Tetracycline (Sigma) and methanol were applied as positive and negative controls, respectively. The MIC value is characterized by the clarity (visible view) of the lowest concentration that represents it. The MBC value is derived from the minimum concentration of the sample that could potentially kill all bacterial cells. The procedure involved applying the MIC and higher concentration treatments onto Mueller-Hinton Agar (MHA; Oxoid) media. The absence of bacterial growth at these concentrations indicates the MBC values. The bacterial strains employed in this study included *B. subtilis* strain M18 and MRSA, both of which were clinical isolates sourced from Dr. Kariadi Central General Hospital, Semarang, Central Java, Indonesia (Agung et al., 2023).

RESULTS AND DISCUSSIONS

Molecular Docking Study Against *B. subtilis* Protein

Molecular docking serves as a structure-based method that examines the interactions between a docked compound and the active site of a protein receptor. This technique provides valuable insights into binding energy and various chemical interactions that may arise during the docking process (Agu et al., 2023). Docking study demonstrated that the binding energies of halogenated thioxanthone derivatives (**TX1**–**TX6**) varied from -6.22 to -7.35 kcal/mol, while tetracycline exhibited a binding energy of -6.63 kcal/mol (**Table 1**). The repositioning of the chloro substituent from the 2-position to the 4-position resulted in a decrease in binding energy, ranging from -6.22 kcal/mol for **TX1** to -6.57 kcal/mol for **TX2**. Furthermore, the addition of one chloro substituent in compounds **TX1** and **TX2** decreased the binding energy from -6.22 and -6.57 to -6.97 kcal/mol in compound **TX3**. Subsequently, switching the bromo substituent from the 2-position to the 4-position resulted in a decrease in binding energy, ranging from -6.40 kcal/mol for **TX4** to -6.78 kcal/mol for **TX5**. The

addition of a bromo substituent decreased the binding energy of compounds **TX4** and **TX5** from -6.40 and -6.78 to -7.35 kcal/mol in compound **TX6**. A comparative analysis of the chloro and bromo substituents based on docking results indicated that the halogenated thioxanthone with the bromo substituent exhibited a lower binding energy its corresponding chloro derivative. A lower binding energy indicates a stronger interaction between the ligand and the protein, signifying enhanced stability and affinity in their interactions (Hari 2019; Nisha et al., 2016).

All halogenated thioxanthone derivatives exhibited interactions with the *B. subtilis* protein through hydrogen bonding, van der Waals forces, carbon-hydrogen interactions, π-sulfur, and π-alkyl interactions (**Figure 2**). The tetracycline formed interactions with Thr247 and Val245 via hydrogen bonding. Additionally, the tetracycline formed interactions with Phe234 and Met254 through alkyl and pi-alkyl interactions. Meanwhile, van der Waals and carbon-hydrogen bond interactions were found between tetracycline and Thr250, Phe251, Leu249, Gly225, Ile222, Val149, Lys246, Glu242, Val241, Phe238, and Asn248. Subsequently, compounds TX3, TX4, and TX6 showed similar hydrogen bonding patterns with the Thr247 amino acids, which were previously found with tetracycline. Compound TX3 demonstrates interactions with Met254 through pi-sigma interactions and with Phe238 via pi-sulfur interactions. In contrast, compound TX6 engages with Val241 through pi-sigma interactions, with Met254 through pi-sulfur interactions, and with Leu249 through halogen interactions. Compounds **TX3** and **TX6**, which demonstrated the lowest binding energy, will undergo further evaluation of their stability through molecular dynamics simulations.

Molecular Docking Study Against DHFR *S. aureus* Protein

The redocking results demonstrated that trimethoprim, used as the native ligand, exhibited an RMSD value of 1.99 Å. Since RMSD values below 2 Å are generally considered indicative of a reliable and reproducible docking protocol, this result confirms the validity of the docking parameters employed (Nivatya et al., 2025). The superimposed structures of the ligand before and after docking are presented in **Figure 3**.

The results of the docking study revealed that the binding energies of halogenated thioxanthone derivatives (**TX1**–**TX6**) varied from -6.93 to -7.65 kcal/mol, while trimethoprim and tetracycline exhibited a binding energy of -7.19 and -7.73 kcal/mol, respectively (**Table 2**). The addition of one chloro substituent in compounds **TX1** and **TX2** decreases the binding energy from -6.93 and -7.34 to -7.65 kcal/mol in compound **TX3.** Subsequently, the addition of a bromo substituent also decreases the binding energy of compounds **TX4** and **TX5** from -7.58 and -7.22 to -7.61 kcal/mol in compound **TX6**. A comparative analysis of the chloro- and bromo-substituted derivatives revealed that both substituents contributed to favorable binding affinities toward the DHFR protein.

Table 1. Molecular docking results of all compounds against *B. subtilis* protein

Compound	Binding Energy (kcal/mol)	Ki	H-Bond
TX1	-6.22	27.8	-
TX2	-6.57	15.31	-
TX3	-6.97	7.81	Thr247
TX4	-6.40	20.44	Thr247
TX5	-6.78	10.81	Ile221
TX6	-7.35	4.12	Thr247
Tetracycline	-6.63	13.91	Thr247, Val245

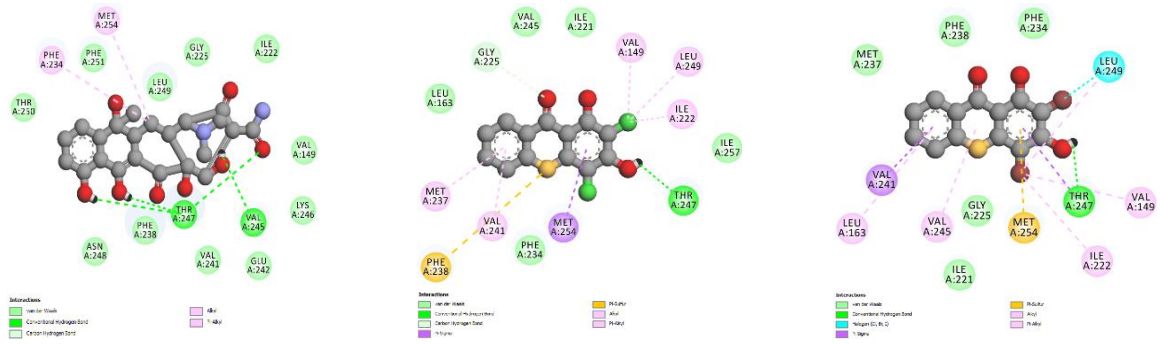

(**a**) (**b**) (**c**)

Figure 2. The interactions (**a**) tetracycline, (**b**) compound **TX3**, and (**c**) compound **TX6** towards *B. subtilis* protein

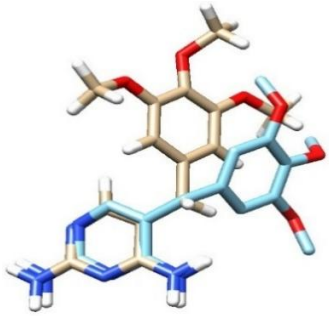

Figure 3. Superimposed structures of the ligand prior to docking (white) and after docking (blue)

Table 2. Molecular docking results of all compounds against DHFR *S. aureus* protein

Compound	Binding Energy (kcal/mol)	Ki	H-Bond
TX1	-6.93	8.32	Asp27, Leu5
TX2	-7.34	4.16	Asp27, Ala7
TX3	-7.65	2.49	Asp27, Ala7, Leu5
TX4	-7.58	2.80	Asp27, Ala7, Leu5
TX5	-7.22	5.07	Ala7
TX6	-7.61	2.65	Asp27, Ala7, Leu5
Trimethoprim	-7.19	5.24	Asp27, Phe92, Leu5
Tetracycline	-7.73	2.17	Asp27, Phe92, Ile14

All halogenated thioxanthone derivatives exhibited interactions with the DHFR protein of *S. aureus* through hydrogen bonding, van der Waals forces, carbon-hydrogen interactions, π-sigma, π-π stacking, and π-alkyl interactions (**Figure 4**). The native ligand trimethoprim formed hydrogen bonds through the amino acid residues of Asp27, Phe92, and Leu5. While tetracycline formed interactions with Phe92, Ile14, and Asp27. Subsequently, compounds **TX1** to **TX6** showed similar hydrogen bonding patterns with the Asp27 amino acids, which were previously found with trimethoprim and tetracycline. Compound **TX3** demonstrated interactions with Thr46 through π-sigma interactions and with Phe92 via π-π stacked interactions. Additionally, compound **TX6** interacted with Phe92 via π-π stacked interactions, with Val31, Leu28, Leu20, and Ile14 through alkyl and π-alkyl interactions. Compounds **TX3** and **TX6**, which exhibited the lowest binding energy, will be further evaluated for their stability using molecular dynamics simulations.

Molecular Dynamics *B. subtilis* Protein

A comprehensive analysis of the top two complexes was carried out through MD simulations over 100 ns to assess their structural stability and dynamic behavior. RMSD quantifies the structural differences in a protein's backbone by comparing its initial conformation to its final position. Protein stability throughout the simulation can be assessed based on the extent of these deviations, with smaller fluctuations indicating greater structural stability (Aier et al., 2016). A lower RMSD value (typically under 2–3 Å for proteins) is often interpreted as a stable conformation. A low RMSD for ligands indicates that the compound remains tightly bound at the active site with no significant alterations or rotations. As presented in Figure 5a, the RMSD values for ligands **TX3**, **TX6**, and tetracycline range between 0.5 and 1.7 Å. These relatively low to moderate fluctuations suggest that each ligand remains stably positioned within its respective binding pocket, undergoing minimal conformational rearrangements throughout the simulation (Jiang et al., 2023; Hassan et al., 2024). Subsequently, the RMSD plot reflects the protein-ligand complexes as a whole, encompassing backbone and side-chain movements of the protein in addition to ligand motion (**Figure 5b**). Throughout the 100 ns molecular dynamics (MD) simulation, compounds **TX6** and tetracycline maintained a consistent RMSD value of 6 Å, whereas compound **TX3** exhibited a fluctuation in RMSD, increasing from 4 Å to 6 Å at approximately 60 ns. These findings suggest that **TX6** demonstrates greater structural stability compared to **TX3**.

In MD simulations, the RMSF serves as a quantitative indicator of a protein structure's flexibility and motion. It assesses the average deviation of atomic positions from their mean over a specified time. Regions exhibiting high RMSF values are anticipated to display greater flexibility, whereas regions with low RMSF values are expected to demonstrate more constrained dynamics[43]. The RMSF graph displayed in **Figure 6a** indicates that the compounds **TX3** and **TX6** exhibited similar amino acid variation patterns to tetracycline. This similarity suggests that these compounds may engage in comparable binding interactions. The RMSF plot further reveals that the complex structures of **TX3**, **TX6**, and tetracycline demonstrate a relatively stable configuration, with an average RMSF value of 2 Å.

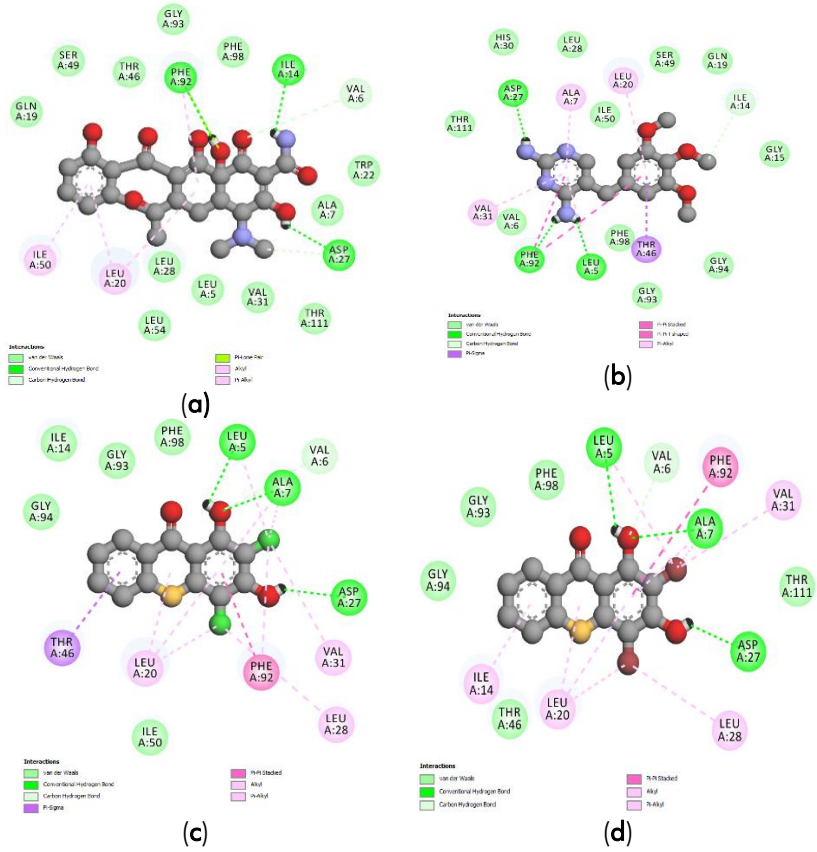

Figure 4. The interactions (**a**) tetracycline, (**b**) trimethoprim, (**c**) compound **TX3**, and (**d**) compound **TX6** towards DHFR *S. aureus* protein

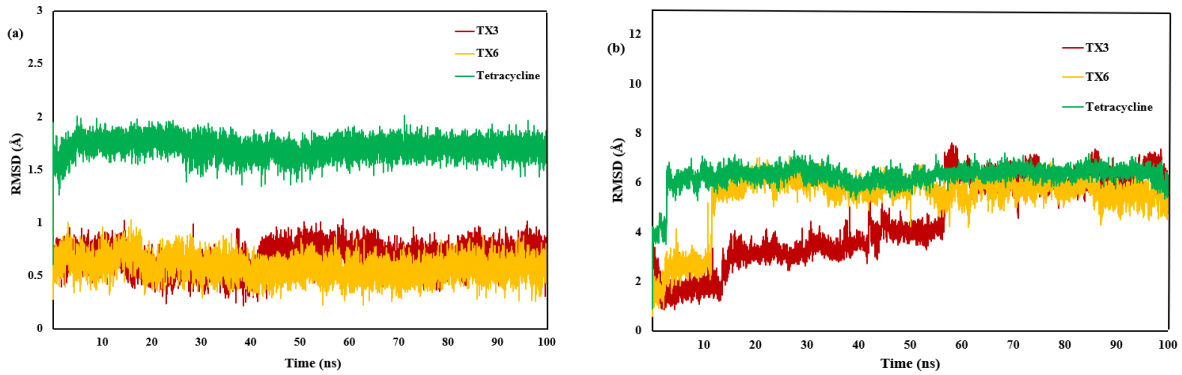

Figure 5. RMSD ligand (**a**) and complex (**b**) for **TX3**, **TX6**, and tetracycline against *B. subtilis* protein

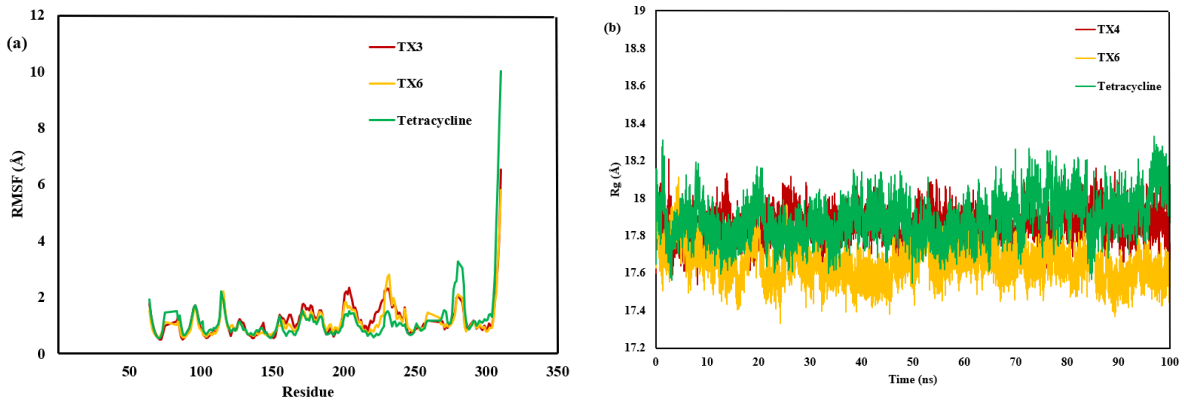

Figure 6. (**a**) RMSF and (**b**) Radius gyration for **TX3**, **TX6**, and tetracycline against *B. subtilis* protein

The Rg serves as a significant metric for assessing the compactness of a protein. It is defined as the root mean square distance of each atom from the protein's center of mass. A smaller Rg value indicates a more compact and globular structure, while a larger Rg value suggests an extended and flexible configuration. This measurement provides valuable insight into the structural properties and dynamics of proteins (Bagewadi et al., 2023). The radius of gyration (Rg) analysis revealed that compounds **TX3**, **TX6**, and tetracycline exhibited consistently stable Rg values with minimal fluctuations, indicating that the proteins retained their structural compactness without significant expansion or contraction (**Figure 6b**).

Molecular Dynamics DHFR *S. aureus* protein

Compounds **TX3** and **TX6** were further evaluated for their stability through molecular dynamics simulations against the DHFR *S. aureus* protein. As illustrated in **Figure 7a**, the RMSD ligand values for compounds **TX3**, **TX6**, and native trimethoprim were consistently 0.5 Å, whereas tetracycline exhibited an RMSD value of 1.7 Å. The low RMSD values observed for all ligands indicate that the compounds remain stably bound to the active site, with minimal structural changes or rotational movement. Subsequently, the RMSD plot provides a comprehensive representation of the protein-ligand complexes, capturing both the conformational changes of the protein's backbone and side chains, along with the movement of the ligand. Over the 100 ns MD simulation, compounds **TX3**, **TX6**, and tetracycline exhibited a stable RMSD value of 3.1 Å, whereas native trimethoprim displayed fluctuations in RMSD within the range of 1 to 2 Å (**Figure 7b**). This finding suggested that compounds **TX3** and **TX6** had similar stability to tetracycline.

The RMSF graph displayed in **Figure 8a** indicates that the compounds **TX3** and **TX6** exhibited similar amino acid variation patterns to tetracycline and trimethoprim. This similarity suggests that these compounds may engage in comparable binding interactions. The RMSF plot demonstrates that the complex structures of **TX3**, **TX6**, and tetracycline maintain a relatively stable conformation, with an average RMSF value of 2 Å. However, compound **TX3** exhibited a notably higher RMSF value in comparison to the other ligands. Subsequently, the Rg analysis revealed that compounds **TX3**, **TX6**, tetracycline, and trimethoprim exhibited consistently stable Rg values of approximately 15.4 Å, with minimal fluctuations. This stability indicates that the proteins maintained their structural compactness, with no significant expansion or contraction observed (**Figure 8b**). Based on the MD simulation results, compounds **TX3** and **TX6** exhibited strong stability, with behavior comparable to that of tetracycline.

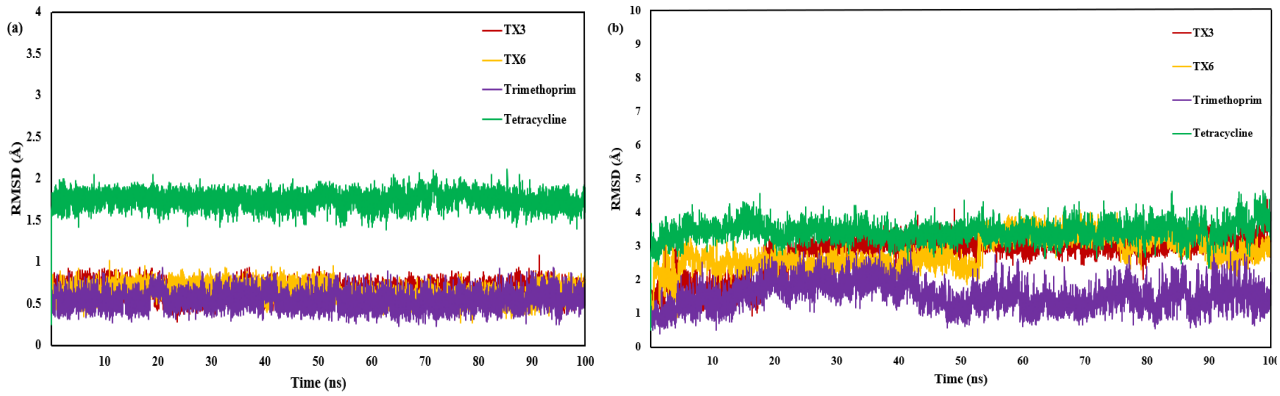

Figure 7. (a) RMSD ligand and (b) complex for **TX3, TX6**, and tetracycline against the DHFR *S. aureus* protein

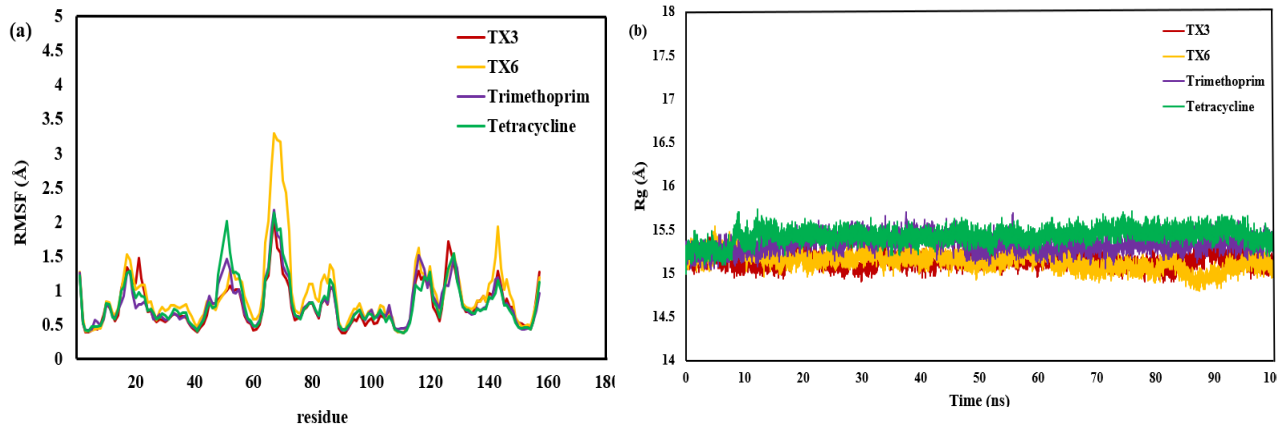

Figure 8. (**a**) RMSF and (**b**) Radius gyration for **TX3**, **TX6**, and tetracycline against DHFR *S. aureus* protein

Table 3. MIC and MBC values for compounds TX3, TX6, and tetracycline

Compound	*B. subtilis* strain M18 clinical isolate		MRSA clinical isolate	
	MIC (μg/mL)	MBC (μg/mL)	MIC (μg/mL)	MBC (μg/mL)
TX3	1.98	3.9	1.98	3.9
TX6	3.9	7.9	3.9	7.9
Tetracycline	3.9	3.9	3.9	3.9

Antimicrobial Activity

The in vitro antibacterial activity of halogenated thioxanthone derivatives **TX3** and T**X6** was assessed against the clinical isolate *B. subtilis* strain M18 and MRSA bacteria. The compounds **TX3** and **TX6** were obtained from our previous study, in which the compounds were synthesized and comprehensively characterized. The molecular structures and purity of **TX3** and **TX6** were confirmed by detailed spectroscopic analyses, including ^{1}H and ^{13}C-NMR, LC–MS, and FTIR. The complete synthetic procedures and full characterization data are reported in that study (Hermawan et al., 2023). The antibacterial efficacy of halogenated thioxanthone derivatives is evaluated through the determination of the MIC and MBC values. The MIC is defined as the lowest concentration of antibiotics or antimicrobials required to effectively inhibit the growth of bacteria (Kowalska & Dudek 2021). On the other hand, MBC has the lowest concentration of an antimicrobial agent that can completely inhibit the growth of bacteria (Mustafa et al., 2018). Compounds **TX3** and **TX6** were found to exhibit antibacterial activity against Gram-positive bacteria *B. subtilis* strain M18 and MRSA. Among the tested compounds, **TX3** exhibited the highest antibacterial activity, with a MIC of 1.98 μg/mL and a MBC of 3.9 μg/mL. In comparison, **TX6** demonstrated a MIC of 3.9 μg/mL and an MBC of 7.9 μg/mL (**Table 3**). The tetracycline exhibited a MIC value of 3.9 μg/mL and MBC value of 3.9 μg/mL. Compound TX3 demonstrated a lower MIC than tetracycline, indicating enhanced antibacterial efficacy. In contrast, compound TX6 exhibited a MIC value comparable to that of tetracycline, suggesting a similar antibacterial potency. However, the higher MBC value of TX6 indicates that a higher concentration was required to achieve bactericidal activity compared with tetracycline. These findings are consistent with the in silico results, which demonstrated that compounds TX3 and TX6 exhibited the lowest binding energies, reflecting strong binding affinity toward the B. subtilis target protein and DHFR from *S. aureus*. This relationship is particularly evident for inhibitory activity (MIC), as molecular docking and molecular dynamics simulations primarily evaluate ligand–target binding interactions.

CONCLUSIONS

The molecular docking analysis against *B. subtilis* protein demonstrated that the halogenated thioxanthone derivatives (TX1–TX6) exhibited binding energies ranging from −6.22 to −7.35 kcal/mol, in comparison to tetracycline, which displayed a binding energy of −6.63 kcal/mol. Additionally, the docking study against DHFR *S. aureus* revealed binding energies for these compounds ranging from −6.93 to −7.65 kcal/mol, whereas trimethoprim and tetracycline exhibited binding energies of −7.19 and −7.73 kcal/mol, respectively. Compounds TX3 and TX6 exhibited the lowest binding energy towards those proteins. The 100 ns molecular dynamics simulation indicated that compounds TX3 and TX6 maintained significant stability when interacting with *B. subtilis* and DHFR *S. aureus* proteins. Based on the antibacterial assay, compound TX3 exhibited the highest antibacterial activity, with a MIC of 1.98 μg/mL and a MBC of 3.9 μg/mL. In comparison, TX6 demonstrated a MIC of 3.9 μg/mL and an MBC of 7.9 μg/mL. The tetracycline exhibited a MIC value of 3.9 μg/mL and MBC value of 3.9 μg/mL. In conclusion, compounds TX3 and TX6 demonstrate promising potential as antibacterial candidates against Gram-positive bacteria.

ACKNOWLEDGEMENTS

The authors gratefully acknowledge the financial support provided by the Ministry of Higher Education, Science, and Technology of the Republic of Indonesia (Kementerian Pendidikan Tinggi, Sains, dan Teknologi) through the Penelitian Dosen Pemula (PDP) research grant under Grant Decree No. 254-15/UN7.D2/PP/IV/2026.

REFERENCES

Agu, P. C., Afiukwa, C. A., Orji, U. O., Ezeh, E. M., Ofoke, I. H., Ogbu, C. O., Ugwuja, E. I., & Aja, P. M. (2023). Molecular docking as a tool for the discovery of molecular targets of nutraceuticals in disease management. *Scientific Reports*, *13*, 13398.

Agung, J., Muhammad, P., Prastya, E., & Indri, R. (2023). The antibacterial and antibiofilm activities of the endophytic bacteria associated with Archidendron pauciflorum against multidrug-resistant strains. *Applied Biochemistry and Biotechnology*, 6653–6674. https://doi.org/10.1007/s12010-023-04382-4

Aier, I., Varadwaj, P., & Raj, U. (2016). Structural insights into conformational stability of both wild-type and mutant EZH2 receptor. *Scientific*

Reports, *6*, 34984. https://doi.org/10.1038/srep34984

Araújo, J., Fernandes, C., Pinto, M., & Tiritan, M. E. (2019). Chiral derivatives of xanthones with antimicrobial activity. *Molecules, 24*(2), 314. https://doi.org/10.3390/molecules24020314

Asyraf, M., Masimen, A., Harun, N. A., & Maulidiani, M. (2022). Overcoming methicillin-resistant Staphylococcus aureus. *Antibiotics, 11*, 1–16.

Bagewadi, Z. K., Yunus Khan, T. M., Gangadharappa, B., Kamalapurkar, A., Mohamed Shamsudeen, S., & Yaraguppi, D. A. (2023). Molecular dynamics and simulation analysis against superoxide dismutase (SOD) target of *Micrococcus luteus* with secondary metabolites from *Bacillus licheniformis* recognized by genome mining approach. *Saudi Journal of Biological Sciences, 30*(9), 103753. https://doi.org/10.1016/j.sjbs.2023.103753

Bernetti, M., & Bussi, G. (2020). Pressure control using stochastic cell rescaling. *Journal of Chemical Physics, 153*(11), 114107. https://doi.org/10.1063/5.0020514

Bessa, L. J., Palmeira, A., Gomes, A. S., Vasconcelos, V., Sousa, E., Pinto, M., & da Costa, P. M. (2015). Synergistic effects between thioxanthones and oxacillin against methicillin-resistant *Staphylococcus aureus*. *Microbial Drug Resistance, 21*, 404–415. https://doi.org/10.1089/mdr.2014.0162

BIOVIA, D. S. (2019). Discovery Studio Visualizer. San Diego, CA.

Bukharie, H. A. (2010). A review of community-acquired methicillin-resistant *Staphylococcus aureus* for primary care physicians. *Journal of Family & Community Medicine, 17*(3), 117–120. https://doi.org/10.4103/1319-1683.74320

Bussi, G., Donadio, D., & Parrinello, M. (2007). Canonical sampling through velocity rescaling. *Journal of Chemical Physics, 126*, 014101.

Darden, T., York, D., & Pedersen, L. (1993). Particle mesh Ewald: An N·log(N) method for Ewald sums in large systems. *Journal of Chemical Physics, 98*(12), 10089–10092.

D'Elia, M. A., Millar, K. E., Bhavsar, A. P., Tomljenovic, A. M., Hutter, B., Schaab, C., Moreno-Hagelsieb, G., & Brown, E. D. (2009). Probing teichoic acid genetics with bioactive molecules reveals new interactions among diverse processes in bacterial cell wall biogenesis. *Chemistry & Biology, 16*, 548–556. https://doi.org/10.1016/j.chembiol.2009.04.009

Durães, F., Palmeira, A., Cruz, B., Freitas-Silva, J., Spengler, G., & Sousa, E. (2021). Antimicrobial activity of a library of thioxanthones and their potential as efflux pump inhibitors. *Pharmaceuticals, 14*(6), 572.

Fatmasari, N., Hermawan, F., Jumina, J., Kurniawan, Y. S., Pranowo, H. D., Puspitasari, A. D., Hastuti, L. P., Marlina, L. A., & Putra, N. R. (2025). Design of hydroxyxanthone derivatives as breast cancer inhibitors: A QSAR modeling, molecular docking, molecular dynamics, MM-PBSA, and ADMET prediction. *Journal of Multidisciplinary Applied Natural Science*, *5*(3). https://doi.org/10.47352/jmans.2774-3047.283

Fuhrmann, J., Rurainski, A., Lenhof, H. P., & Neumann, D. (2010). A new Lamarckian genetic algorithm for flexible ligand-receptor docking. *Journal of Computational Chemistry, 31*(9), 1911–1918. https://doi.org/10.1002/jcc.21478

Gampa, M., Padmaja, P., & Khalivulla, S. I. (2022). Synthesis and antimicrobial and antioxidant activities of 1,2,3-triazole-tethered xanthone derivatives. Russian *Journal of Organic Chemistry, 58*, 872–877. https://doi.org/10.1134/S1070428022060173

Haque, M. A., Hu, H., Liu, J., Islam, M. A., & Hossen, F. (2024). Emergence of multidrug-resistant Bacillus spp. derived from animal feed, food and human diarrhea in South-Eastern Bangladesh. *BMC Microbiology*, *24*, 6.

Hari, S. (2019). In silico molecular docking and ADME/T analysis of plant compounds against IL17A and IL18 targets in gouty arthritis. *Journal of Applied Pharmaceutical Science, 9*(7), 018–026.

Hassan, A. M., Gattan, H. S., Faizo, A. A., Alruhaili, M. H., Alharbi, A. S., Bajrai, L. H., Al-Zahrani, I. A., Dwivedi, V. D., & Azhar, E. I. (2024). Evaluating the binding potential and stability of drug-like compounds with the monkeypox virus VP39 protein using molecular dynamics simulations and free energy analysis. *Pharmaceuticals*, *17*(12), 1617. https://doi.org/10.3390/ph17121617

Hastuti, L. P., Hermawan, F., Iresha, M. R., Ernawati, T., & Firdayani. (2024). In silico studies of hydroxyxanthone derivatives as potential pfDHFR and pfDHODH inhibitors by molecular docking, molecular dynamics simulation, MM-PBSA calculation and pharmacokinetics prediction. *Informatics in Medicine Unlocked*, *47*. https://doi.org/10.1016/j.imu.2024.101485

Hermawan, F., Jumina, J., Ernawati, T., Asih, P. B. S., Rozi, I. E., Coutrier, E. F. N., & Syafruddin, D. (2024). Molecular docking, molecular dynamics simulation, and in vitro evaluation of hydroxythioxanthone derivatives as antimalarial agents. *The Thai Journal of Pharmaceutical Sciences*, *48*(4).

Hermawan, F., Jumina, J., Pranowo, H. D., Sholikah, E. N., Ernawati, T., & Azminah, A. (2023). In

silico approach for design, synthesis and biological evaluation of thioxanthone derivatives as potential anticancer agents. *ChemistrySelect*, e202304014. https://doi.org/10.1002/slct.202304014

Hess, B., Kutzner, C., van der Spoel, D., & Lindahl, E. (2008). GROMACS 4: Algorithms for highly efficient, load-balanced, and scalable molecular simulation. *Journal of Chemical Theory and Computation, 4*(3), 435–447. https://doi.org/10.1021/ct700301q

Huang, J., & MacKerell, A. D., Jr. (2013). CHARMM36 all-atom additive protein force field: Validation based on comparison to NMR data. *Journal of Computational Chemistry, 34*(25), 2135–2145. https://doi.org/10.1002/jcc.23354

Iresha, M., Jumina, J., Pranowo, H., Sholikhah, E., & Hermawan, F. (2022). Synthesis, cytotoxicity evaluation and molecular docking studies of xanthyl-cinnamate derivatives as potential anticancer agents. *Indonesian Journal of Chemistry, 22*(5), 1407–1417. http://dx.doi.org/10.22146/ijc.76164

Jiang, T., Chen, X., Yang, W., Li, N., Jinhong, X., Yang, L., Sisi, Z., Shuihong, Y., & Li, Y. (2023). Network pharmacology, molecular docking, molecular dynamics simulation, and in vitro experiments to explore the mechanism of asiatic acid inhibiting acetaldehyde-induced activation of hepatic stellate cells. *Natural Product Communications*, *18*(8). https://doi.org/10.1177/1934578X231194127

Kawai, Y., Marles-Wright, J., Cleverley, R. M., Emmins, R., Ishikawa, S., Kuwano, M., Heinz, N., Bui, N. K., Hoyland, C. N., Ogasawara, N., Lewis, R. J., Vollmer, W., Daniel, R. A., & Errington, J. (2011). A widespread family of bacterial cell wall assembly proteins. *The EMBO Journal, 30*, 4931–4941. https://doi.org/10.1038/emboj.2011.358

Kowalska-Krochmal, B., & Dudek-Wicher, R. (2021). The minimum inhibitory concentration of antibiotics: Methods, interpretation, and clinical relevance. *Pathogens*, *10*(2), 165. https://doi.org/10.3390/pathogens10020165

Kumar, A., Singh, K. A., Thareja, S., & Kumar, P. A. (2023). Review of pyridine and pyrimidine derivatives as anti-MRSA agents. *Anti-Infective Agents, 21*, 18–40. https://doi.org/10.2174/2211352520666220705085733

Lakhundi, S., & Zhang, K. (2018). Methicillin-resistant *Staphylococcus aureus*: Molecular characterization. *Clinical Microbiology Reviews*, *32*. https://doi.org/10.1128/CMR.00020-18

Librowski, T., Czarnecki, R., Czekaj, T., & Marona, H. (2005). New xanthone derivatives as potent anti-inflammatory agents. *Medicina (Kaunas), 41*, 54–58.

Lu, Y., Guan, T., Wang, S., Zhou, C., Wang, M., Wang, X., Zhang, K., Han, X., Lin, J., Tang, Q., Wang, C., & Zhou, W. (2023). Novel xanthone antibacterials: Semi-synthesis, biological evaluation, and the action mechanisms. *Bioorganic & Medicinal Chemistry, 83*, 117232. https://doi.org/10.1016/j.bmc.2023.117232

Morris, G. M., Huey, R., Lindstrom, W., Sanner, M. F., Belew, R. K., Goodsell, D. S., & Olson, A. J. (2009). AutoDock4 and AutoDockTools4: Automated docking with selective receptor flexibility. *Journal of Computational Chemistry, 30*(16), 2785–2791. https://doi.org/10.1002/jcc.21256

Mustafa, H., Ismail, N., & Wahab, W. N. A. W. A. (2018). Antimicrobial activity of aqueous *Quercus infectoria* gall extract against pathogenic Leptospira. *Malaysian Journal of Medical Sciences, 25*(4), 42–50. https://doi.org/10.21315/mjms2018.25.4.4.

Nakagawa, Y., Inomata, A., Moriyasu, T., & Suzuki, T. (2020). Cytotoxic effects of thioxanthone derivatives as photoinitiators on isolated rat hepatocytes. *Journal of Applied Toxicology, 40*, 234–244.

Neese, F. (2018). Software update: The ORCA program system, version 4.0. Wiley Interdisciplinary Reviews: *Computational Molecular Science, 8*, 1–6. https://doi.org/10.1002/wcms.1327

Nisha, C. M., Kumar, A., Nair, P., Gupta, N., Silakari, C., Tripathi, T., & Kumar, A. (2016). Molecular docking and in silico ADMET study reveals acylguanidine 7a as a potential inhibitor of β-secretase. *Advances in Bioinformatics*, 1–6. https://doi.org/10.1155/2016/9258578

Nivatya, H. K., Singh, A., Kumar, N., Sonam, Lovy S., Vishal S., Raghav M., Nishant G., Arun K.M. (2025). Assessing molecular docking tools: Understanding drug discovery and design. *Future Journal of Pharmaceutical Sciences*, *11*, 111. https://doi.org/10.1186/s43094-025-00862-y

Pedrola, M., Jorba, M., Jardas, E., Jardí, F., Ghashghaei, O., Viñas, M., & Lavilla, R. (2019). Multicomponent reactions upon the known drug trimethoprim as a source of novel antimicrobial agents. *Frontiers in Chemistry, 7*, 1–9. https://doi.org/10.3389/fchem.2019.00475

Pettersen, E. F., Goddard, T. D., Huang, C. C., Couch, G. S., Greenblatt, D. M., Meng, E. C., & Ferrin, T. E. (2004). UCSF Chimera—A visualization system for exploratory research and analysis. *Journal of Computational Chemistry, 25*, 1605–1612. https://doi.org/10.1002/jcc.20084

Proença, C., Albuquerque, H., Ribeiro, D. M., Freitas, M., Santos, C., Silva, A., & Fernandes, E.

(2016). Novel chromone and xanthone derivatives: Synthesis and ROS/RNS scavenging activities. *European Journal of Medicinal Chemistry, 115*, 381–392. https://doi.org/10.1016/j.ejmech.2016.03.043

Putra, R. H., Retnowati, D. W. I., Cordova, D. M., Azkia, A., Primahana, G., Dewi, R. T., Filailla, E., & Eka, M. (2024). Antibacterial and antioxidant properties of bioactive compounds derived from endophytic bacteria isolated from nyatoh (*Palaquium amboinense* B.). *Jurnal Sumberdaya Hayati, 10*, 25–32. https://doi.org/10.29244/jsdh.10.1.25-32

Resende, D. I. S. P., Pereira-Terra, P., Moreira, J., Freitas-Silva, J., Lemos, A., Gales, L., Inácio, A. S., da Costa, P. M., Pinto, E., Sousa, E., & Pinto, M. M. M. (2020). Synthesis of a small library of nature-inspired xanthones and study of their antimicrobial activity. *Molecules, 25*, 1–20. https://doi.org/10.3390/molecules25102405

Resende, D. I. S. P., Pereira-Terra, P., Inácio, A. S., da Costa, P. M., Pinto, E., Sousa, E., & Pinto, M. M. M. (2018). Lichen xanthones as models for new antifungal agents. *Molecules*, *23*. https://doi.org/10.3390/molecules23102617

World Health Organization. (2023). Antimicrobial resistance expected to cause 5.2 million deaths in the Western Pacific by 2030. Retrieved from https://www.who.int/westernpacific/news/item/13-06-2023-antimicrobial-resistance-expected-to-cause-5.2-million-deaths-in-the-western-pacific-by-2030